On the decompression melting structure at volcanic arcs and back-arc spreading centers

James A. Conder, Douglas A. Wiens, and Julie Morris

Department of Earth and Planetary Sciences, Washington University, St. Louis, Missouri, USA

Received 26 April 2002; revised 13 June 2002; accepted 21 June 2002; published 6 August 2002.

[1] Mantle dynamics can strongly affect melting processes beneath spreading centers and volcanic arcs. A 2-D numerical model of the Tonga subduction zone, with the slab viscously coupled to the mantle beneath the brittle-ductile transition but faulted above, shows that induced corner flow may cause asymmetric melting at the Lau back-arc spreading center, 400 km away. The down-going slab also entrains the high-viscosity base of the overlying lithosphere, drawing hot, low-viscosity asthenosphere upwards into the gap, triggering decompression melting in the wedge. Because the slab is decoupled from the brittle overlying plate, a cold upper corner develops, inhibiting melting where the slab is shallow. The cold corner is consistent with seismic attenuation and heat flow at arcs. Decompression melting may be a substantial fraction of magma production at some arcs, but less at others. Possibly more important, the shallow decompression melting structure may govern the pathways of melt extraction beneath volcanic arcs. *INDEX TERMS:* 8120 Tectonophysics: Dynamics of lithosphere and mantle—general; 8123 Tectonophysics: Dynamics, seismotectonics; 8439 Volcanology: Physics and chemistry of magma bodies; 9355 Information Related to Geographic Region: Pacific Ocean; 3230 Mathematical Geophysics: Numerical solutions

1. Introduction

[2] Recent research has challenged previous views about melt production and structure beneath oceanic spreading centers and volcanic arcs. Magma beneath volcanic arcs is typically thought to be generated by the subducting plate releasing water into the overlying mantle wedge [e.g., *Tatsumi*, 1986]. Hydration melting is an attractive mechanism because it explains the apparent contradiction of melting in the cold, downwelling environment near a subducting slab. Melt inclusions in early crystallized minerals can contain as much as 6 wt% H_2O, consistent with hydration melting [*Sisson and Layne*, 1993]. However, some melt inclusions contain <0.4 wt% H_2O and high amounts of CO_2, indicating that some melting at arcs is nearly anhydrous and suggesting that decompression melting may occur in an arc setting [*Sisson and Bronto*, 1998].

[3] Mid-ocean ridge volcanism has been thought to be generated by symmetric upwelling and subsequent decompression melting of mantle beneath the ridge. The MELT experiment, designed to detect melt beneath the East Pacific Rise (EPR), showed a pronounced asymmetry in geophysical properties about the EPR indicative of an asymmetric melting structure [*MELT*, 1998]. This asymmetry may be a result of asthenospheric flow across the ridge [*Conder et al.*, 2002]. A recent seismic experiment across the Lau back-arc spreading center in the Lau Basin also suggests an asymmetric melting structure about the spreading center with more melt to the west [*Zhao et al.*, 1997] (Figure 1), possibly indicating across-axis mantle flow near the spreading center. Beneath the Tonga arc, there is an extensive, seismically slow region above and paralleling the slab that likely indicates of the presence of melt (Figure 1). With finite-element viscous flow models, we examine the mantle dynamics that govern the decompression melting structure in the arc and back-arc environments. In particular, we determine that (1) decompression melting in arcs is a likely response to thermal and viscous erosion of the base of the overriding plate associated with corner flow induced by the subducting slab, (2) the asymmetric melt structure in the Lau back-arc is likely caused by a west-to-east across-axis asthenospheric flow induced by the subducting slab and (3) back-arc spreading may significantly affect melting at the arc.

2. Numerical Model

[4] We examine dynamics in the mantle wedge with a 121 × 81 node finite-element viscous flow model with temperature- and pressure-dependent viscosity and variable node spacing to give the best resolution in the wedge corner. We pattern our model after the Tonga subduction zone. The model is 500 km wide and 400 km deep with stress-free boundary conditions on the sides and bottom of the box and velocity conditions along the top and in the upper slab. In the trench-fixed reference frame, the overriding plate is stationary. The slab begins with the temperature structure of an 80-Myr-old plate, and descends at a 45° dip at a rapid convergence rate of 180 mm/yr [*Bevis et al.*, 1995] (we ignore the shallower dip at <40 km depth). Because a viscous flow assumption is not realistic for lithosphere above the brittle-ductile transition, all nodes colder than 800°C in the overriding plate are assigned a rigid kinematic condition, rather than allowed to deform viscously (i.e., velocity = 0 in the overriding plate). A colder transition in the mantle wedge makes more of the overlying plate behave viscously, enhancing decompression melting in the wedge relative to that discussed below and shifting the entire melting structure a few 10s of km trenchward. To model decompression melting beneath the arc and back-arc we use a depletion-dependent melting function previously used in a mid-ocean ridge setting [*Jha et al.*, 1994], which calculates the melt production rate of a parcel of mantle based on its temperature, depth, previous melting history, and upwelling rate, assuming a normal MORB source starting mantle

0094-8276/02/2002GL015390$05.00

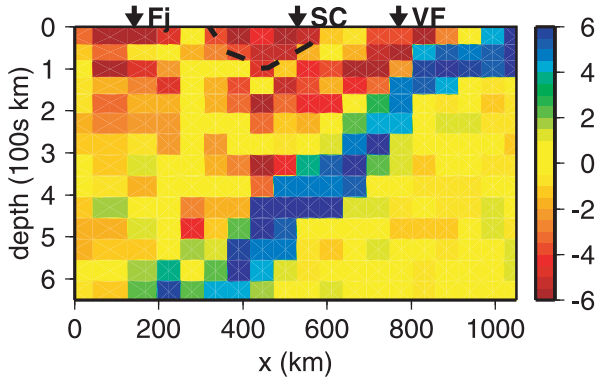

Figure 1. P-wave velocity structure beneath the Lau back-arc basin. After *Zhao et al.* [1997]. Nodes in the Zhao et al. model are represented by blocks. Resolution is close to the node spacing. Colors denote % P-wave velocity deviation from IASP91. Blue colors denote fast, likely cold, regions such as the subducting slab. Red denotes slow velocities likely indicating the presence of melt and/or high temperatures. Main regions of slow velocity are 1) beneath Fiji (Fj), 2) an asymmetric region beneath the Lau back-arc spreading center (SC) (dashed outline), and 3) beneath the volcanic front (VF) and above the subducting slab.

composition. For further details of the modeling see *Conder et al.* [2002].

3. Results

3.1. Arc

[5] In the model, the slab is decoupled from the overriding plate where the overriding plate is assumed to behave elastically and faulting accommodates permanent deformation. Below the brittle-ductile transition, the slab is viscously coupled to the surrounding mantle. Rapid cooling occurs in the uppermost corner of the wedge from both its proximity to the surface and constant juxtaposition with the coldest portion of the down-going slab. In our model, this cooling maintains the brittle rheology of the fault separating the down-going slab and the overriding plate to depths ~50 km, consistent with the 40 km depth suggested by the lower edge of the seismogenic plate interface [*Ruff and Tichelaar*, 1996], and the 50–60 km depth of the aseismic front, where forearc earthquakes cease to occur [*Hasegawa et al.*, 1994].

[6] Decompression melting can occur beneath the arc as the descending slab ablates the lower (viscously deformable) portion of the overiding plate (Figure 2). As the overriding plate thins near the slab, high-temperature, low-viscosity asthenosphere is drawn in to fill the gap, adding heat to the corner, and further thinning the lithosphere. As hot, low-viscosity asthenosphere upwells into the corner, melting is triggered by decompression. The amount of decompression melting generated at the arc depends somewhat on the subduction rate, with greater subduction rates generating larger amounts of melting. Even at high subduction rates, the upwelling, hot asthenosphere cannot penetrate the rigid overlying plate to the uppermost regions of the cold corner, so melting ceases where the slab is roughly 80 km below the surface (Figure 2). However, the melting region stretches laterally over where the slab reaches nearly 200 km depth, with the bulk occurring where the slab is closer to 110 km deep (Figure 2). This mechanism is consistent with the observation that arc volcanoes consistently appear at the surface where the slab reaches ~90–120 km depth and that the across-arc volcano distribution is asymmetric with fewer volcanoes and smaller spacing toward the forearc than the back-arc [*Tatsumi*, 1986; *Tatsumi and Eggins*, 1995]. Because decompression melting occurs in the uppermost mantle wedge, it may govern the pathways for melt extraction of deeper hydration melting beneath arcs, particularly if melt is extracted through a network of reaction channels [*Kelemen et al.*, 1995] or coalescing diapirs [*Hall and Kincaid*, 2001]. This may help explain the ubiquity of arcs occurring ~90–120 km above the slab even though hydrous minerals may not completely breakdown until 150–250 km depth [*Schmidt and Poli*, 1998].

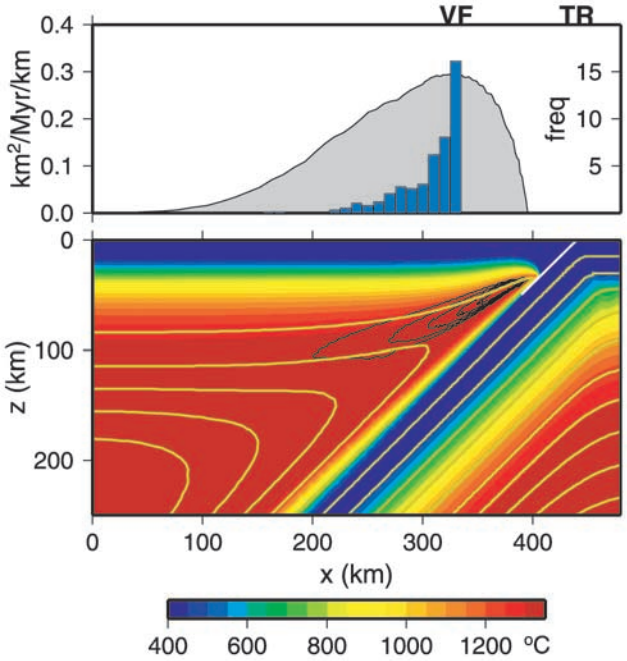

Figure 2. Calculated temperature (colors) and decompression melting rate (unfilled contours) above a fast subducting slab, assuming a MORB source mantle. Contours are in increments of 0.2%/Myr, with the highest values of 1%/Myr in the uppermost corner. Because of the strong dependence on the assumed solidus, absolute values of melt production are less robust than the relative values. Yellow-green lines are streamlines. Ablation of the lower portion of the upper plate by the subducting slab draws hot, low-viscosity asthenosphere upwards into the gap, triggering decompression melting. Upper panel shows the predicted distribution of volcanism if all the melt produced in the lower panel rose buoyantly to the surface with no focusing. Area under the curve sums to ~25 km^3/My per km of arc. Volcanism gets no closer to the trench (TR) than where the slab is 80 km deep, with the peak of volcanism (VF) occurring at ~110 km above the slab. Histogram shows the frequency distribution between individual volcanoes in oceanic arcs and their relation to the volcanic front. An asymmetric melt distribution will likely lead to an asymmetric volcano distribution. Frequency data from [*Tatsumi and Eggins*, 1996].

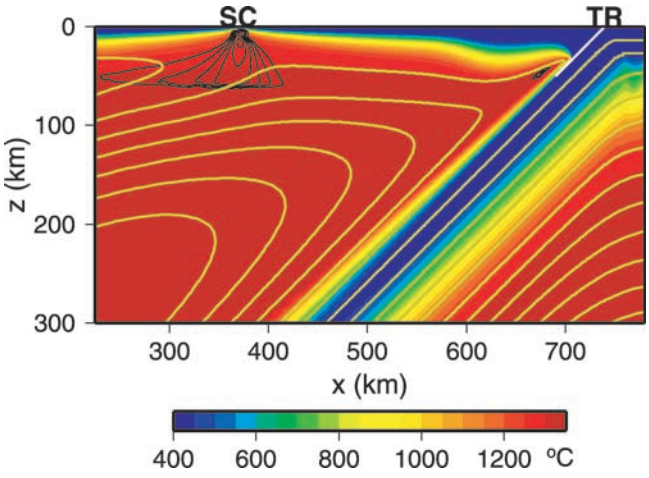

Figure 3. Calculated temperature and decompression melting structure scaled for the Lau back-arc basin with a back-arc spreading center. Shading and contours same as in Figure 2. Contours beneath the spreading center (SC) are in increments of 3%/Myr, with the greatest productivity just beneath the axis. Small, closed contour beneath the arc is 0.1%/Myr. Because of the across-axis flow induced from the subducting slab, melting in the back-arc is highly asymmetric, with more melt to the west. Considerably less melting occurs beneath the arc, because wedge material is fed from the west, where it has been previously depleted from melting at the back-arc spreading center.

[7] Viscous ablation of the overriding lithosphere was suggested as a possible mechanism for melting at arcs more than 25 years ago, as it became apparent that melting from frictional heating is unlikely at arcs [*Sleep*, 1975], but the idea was never fully explored and has been largely ignored by more recent studies for two main reasons. First, melting from hydration of the wedge explains much of the chemistry of arc lavas and probably does generate a significant portion of arc magmas, so alternative mechanisms have not been pursued. Second, many subduction modeling studies have used an isoviscous rheology or other assumptions, such as weak nodes at the fault interface that hindered ablation, so it was not often observed. All analytic models use an isoviscous mantle structure, as a variable viscosity flow structure requires a numerical solution. Many numerical studies also use an isoviscous structure to simplify the calculations. While an isoviscous assumption poses little problem over most of the model space, processes such as viscous and thermal erosion of the base of the overlying plate are not adequately modeled. For practical reasons, laboratory models are nearly always isoviscous or have one discrete viscosity contrast between the lithosphere and asthenosphere, again inhibiting processes such as ablation of the lower lithosphere that may be important in real arcs.

[8] Different formulations have been used in variable-viscosity numerical models to decouple the overriding and subducting plates, with differing results. Variable-viscosity models that assume the two plates are completely viscously coupled show a dramatic amount of ablation of the overriding plate, with hot, upwelling asthenosphere kept from reaching the surface only because of the assigned boundary conditions, leading to dramatic over-predictions of heat flow in the forearc and arc [*Rowland and Davies*, 1999; *Eberle et al.*, 2002]. Dynamic models often incorporate weak (low-viscosity) nodes at the subduction-overriding plate interface to keep the two plates from simply thickening, or underplating each other [e.g., *Kincaid and Sacks*, 1997]. Although coupling is reduced, the weak-node formulation still has some shallow coupling between the two plates, so the weak nodes are usually extended much deeper than the seismogenic fault zone, likely changing the appropriate amount of viscous coupling at depth and resulting in a poor fit to the heat flow at the arc and the seismic velocity structure in the wedge [*Eberle et al.*, 2002].

3.2. Back-Arc

[9] To include the back-arc spreading center, we expand the model to 800 km width and add 60 nodes in the horizontal direction. We initiate back-arc spreading after the slab has reached steady state. The overriding plate is still stationary, but grows laterally as the spreading center migrates to the west at the half-spreading rate, while the plate west of the spreading center moves to the west at the full-spreading rate of 80 mm/yr [*Zellmer and Taylor*, 2001].

[10] As the slab descends, the surrounding viscous mantle is dragged down with it, imposing a corner flow throughout the system. The corner flow fundamentally alters the upwelling pattern at the back-arc spreading center several hundreds of kilometers away (Figure 3) by imposing a west-to-east across-axis flow at the spreading center. Because the lithosphere slopes in opposite directions from the spreading center, across-axis flow causes an asymmetric melting structure with more upwelling and melting to the west as asthenosphere travels up the sloping lithosphere towards the axis and less upwelling and melting on the eastern side as the thickening lithosphere forces the asthenosphere downward. The case shown here (Figure 3) exhibits more than 3$\times$ more melting on the western side than the eastern side of the axis. Trench-parallel flow is likely important at many arcs, including Tonga, as demonstrated by seismic anisotropy studies [*Smith et al.*, 2001]. However, the observed asymmetric slow velocity region beneath the back-arc spreading center implies that corner flow is important to mantle dynamics at subduction zones and may act in concert with trench-parallel flow.

[11] The presence of a back-arc spreading center also alters the melting structure beneath the arc. If the spreading center and the arc melting regimes are close enough, such as in the Valu Fa or southern Marianas, the melts may mix or be diverted to the other outlet [e.g., *Martinez and Taylor*, 2002]. In our model, the spreading center is far enough away that the two melting regimes are spatially separated, but still the presence of the spreading center reduces the amount of melting beneath the arc. Because of the overall corner flow pattern, mantle material is delivered to the wedge that has been previously depleted at the spreading center (Figure 3), so the amount of melting at the arc is accordingly reduced (in our model it is reduced from 25 to <2 km^3/Myr/km). The melting in Figure 2 occurs with small amounts of water present (comparable to MORB source material), and the amount of melting becomes minimal when water is previously extracted at the spreading center. However, we note that the melting occurs close to the dry solidus, so small differences in mantle composition or temperature can lead to large differences in melt production. Mantle temperatures and composition may vary between arcs, so the amounts of

decompression melting could vary considerably. Whatever the mantle characteristics in a particular arc-back-arc system, back-arc spreading likely reduces the amount of melting at the arc relative to what it was before spreading was initiated.

4. Discussion

[12] The subduction and back-arc model developed in this paper explains many geophysical and geochemical observations at arcs and back-arcs. The induced across-axis flow implies that asthenosphere is drawn to the mantle wedge from the back-arc spreading center. A flow pattern where asthenosphere that has been previously melted at the ridge is drawn to the melting region beneath the arc easily explains the consistently greater depletion often observed in arc basalts relative to their associated back-arc basalts [e.g., *McCulloch and Gamble*, 1991]. This relationship has been particularly noted in Tonga arc basalts, where greater depletion correlates with local back-arc spreading rates [*Ewart and Hawkesworth*, 1987]. The reduced degree of melting at the arc because of previous depletion also explains the small size of the active Tofua arc (just west of the Tonga Ridge). When rifting began in Tonga, it split the previously active arc into the present-day inactive Tonga and Lau Ridges [*Shipboard Scientific Party*, 1992]. A simple calculation based on the volume of material above 2000 m depth on the seafloor shows that the Tonga and Lau Ridges contain about 100× more crustal material than the Tofua arc. The previous arc was active for nearly ten times longer [*Shipboard Scientific Party*, 1992], suggesting a reduction of nearly one order of magnitude in arc production after rifting began.

[13] A subducting slab model that is viscously coupled beneath the brittle-ductile transition, but decoupled above it, results in viscous and thermal erosion of the lower lithosphere of the overriding plate and the development of a cold upper corner. The cold corner, where cooling from the surface and the subducting slab inhibits the flow of warm asthenosphere further into the corner, creates a nearly vertical boundary between hot asthenosphere beneath the arc and cold, rigid material towards the trench. A boundary between high temperature material beneath the arc and cold temperature material beneath the forearc has been suggested on the basis of heat flow [*Honda*, 1985; *Furukawa*, 1993] and seismic attenuation [*Research Group for Explosion Seismology*, 1977]. That the model presented here qualitatively matches the seismic structure in Figure 1 and other geophysical and geochemical data suggests that slab induced mantle flow coupled just beneath the brittle-ductile transition significantly affects the melting structure in both the arc and back-arc environments.

[14] **Acknowledgments.** We thank Michael Eberle for sharing his work prior to publication. We thank Norm Sleep and an anonymous reviewer for their comments and criticisms, which improved the quality of this paper. This work was supported by the National Science Foundation grant #s OCE-0002527 and EAR-9614502.

References

Bevis, M., F. W. Taylor, B. E. Schultz, J. Recy, B. L. Isacks, S. Hely, R. Singh, E. Kendrick, J. Stowell, B. Taylor, and S. Calmont, Geodetic observations of very rapid convergence and back-arc extension at the Tonga arc, *Nature*, *374*, 249–251, 1995.

Conder, J. A., D. W. Forsyth, and E. M. Parmentier, Asthenospheric flow and the asymmetry of the East Pacific Rise, MELT area, submitted, 2002.

Eberle, M. A., O. Grasset, and C. Sotin, A numerical study of the interaction between the mantle wedge, subducting slab and over-riding plate, *Phys. Earth and Plan. Int.*, in press, 2002.

Ewart, A., and K. D. Hawkesworth, The Pleistocene-recent Tonga-Kermadec arc lavas: Interpretation of new isotopic and rare Earth data in terms of a depleted mantle source model, *J. Petrol.*, *28*, 495–530, 1987.

Furukawa, Y., Depth of the decoupling interface and thermal structure under arcs, *J. Geophys. Res.*, *98*, 20,005–20,013, 1993.

Hall, P. S., and C. Kincaid, Diapiric flow at subduction zones: A recipe for rapid transport, *Science*, *292*, 2472–2475, 2001.

Hasegawa, A., S. Horiuchi, and N. Umino, Seismic structure of the northeastern Japan convergent margin: A synthesis, *J. Geophys. Res.*, *99*, 22,295–22,311, 1994.

Honda, S., Thermal structure beneath Tohoku, northeast Japan—A case study for understanding the detailed thermal structure of the subduction zone, *Tectonophysics*, *112*, 69–102, 1985.

Jha, K., E. M. Parmentier, and J. Phipps Morgan, The role of mantle-depletion and melt-retention buoyancy in spreading-center segmentation, *Earth Planet. Sci. Lett.*, *125*, 221–234, 1994.

Kelemen, P. B., N. Shimizu, and V. J. M. Salters, Extraction of mid-ocean ridge basalt from the upwelling mantle by focused flow of melt in dunite channels, *Nature*, *375*, 747–753, 1995.

Kincaid, C., and I. S. Sacks, Thermal and dynamical evolution of the upper mantle in subduction zones, *J. Geophys. Res.*, *102*, 12,295–12,315, 1997.

Martinez, F., and B. Taylor, Mantle wedge control on back-arc crustal accretion, *Nature*, *416*, 417–420, 2002.

McCulloch, M. T., and J. A. Gamble, Geochemical and geodynamical constraints on subduction zone magmatism, *Earth Planet. Sci. Lett.*, *102*, 358–374, 1991.

MELT Seismic Team, Imaging the deep seismic structure beneath a mid-ocean ridge: The MELT experiment, *Science*, *280*, 1215–1218, 1998.

Research Group for Explosion Seismology, Regionality of the upper mantle around northeastern Japan as derived from explosion seismic observations and its seismological implications, *Tectonophysics*, *37*, 117–130, 1977.

Rowland, A., and J. H. Davies, Buoyancy rather than rheology controls the thickness of the overriding mechanical lithosphere at subduction zones, *Geophys. Res Lett.*, *19*, 3037–3040, 1999.

Ruff, L. J., and B. W. Tichelaar, What controls the seismogenic plate interface in subduction zones?, in *Subduction Top to Bottom, AGU Monogr. 96*, edited by G. E. Bebout, D. W. Scholl, S. H. Kirby, and J. P. Platt, pp. 105–111, 1996.

Schmidt, M. W., and S. Poli, Experimentally based water budgets for dehydrating slabs and consequences for arc magma generation, *Earth Planet. Sci. Lett.*, *163*, 361–379, 1998.

Shipboard Scientific Party, Introduction, background, and principal results of Leg 135, Lau Basin, *Proc. Ocean Drill. Program Initial Rep.*, *135*, 5–47, 1992.

Sisson, T. W., and S. Bronto, Evidence for pressure-release melting beneath magmatic arcs from basalt at Galunggung, Indonesia, *Nature*, *391*, 883–886, 1998.

Sisson, T. W., and G. D. Layne, H_2O in basalt and basaltic andesite glass inclusions from four subduction-related volcanoes, *Earth Plan. Sci. Lett.*, *117*, 619–635, 1993.

Sleep, N., Stress and flow beneath island arcs, *Geophys. J. R. Astr. Soc.*, *42*, 827–857, 1975.

Smith, G. P., D. A. Wiens, K. M. Fischer, L. M. Dorman, S. C. Webb, and J. A. Hildebrand, A complex pattern of mantle flow in the Lau backarc, *Science*, (292), 713–716, 2001.

Tatsumi, Y., Formation of the volcanic front in subduction zones, *Geophys. Res Lett.*, *13*, 717–720, 1986.

Tatsumi, Y., and S. M. Eggins, Subduction Zone Magmatism, Blackwell Science, edited by Y. Tatsumi, 1995.

Zellmer, K. E., and B. Taylor, A three-plate kinematic model for Lau basin opening, *G-cubed*, *2*, #2000GC000106, 2001.

Zhao, D., Y. Xu, D. A. Wiens, L. Dorman, J. Hildebrand, and S. Webb, Depth extent of the Lau back-arc spreading center and its relation to the subduction process, *Science*, *278*, 254–257, 1997.

J. A. Conder, J. Morris, and D. A. Wiens, Department of Earth and Planetary Sciences, Washington University, Box 1169, St. Louis, MO 63130, USA. (conder@seismo.wustl.edu)